Predicting oil sands viscosity from well logs using an industry provided dataset

Eric A. Rops and Laurence R. Lines

ABSTRACT

This study is an expansion of the work the author did in the previous CREWES report (Rops & Lines 2015), where it was demonstrated that heavy oil viscosity could be predicted directly from well logs within 25% error using a limited dataset. To further explore this idea, Donor Company has generously provided viscosity data from their Athabasca North and Athabasca South oil sands development projects, with multiple measurements per well.

Multi-attribute analysis enables a target attribute (viscosity) to be predicted using other known attributes (the well logs). In the Athabasca North area, *P-wave sonic* and *Density porosity* were used to predict viscosity and the average validation error was 147,000cP, or 19% of the total viscosity range. In the Athabasca South area, *medium resistivity, gamma ray,* and *P-wave sonic* were used to predict viscosity and the average validation error was only 70,000 cP, or 13% of the total viscosity range.

INTRODUCTION

Most of the world's oil resources are heavy, viscous hydrocarbons that are difficult and costly to produce and refine. With high oil prices and demand, and production of most conventional-oil reservoirs in decline, industry focus in many parts of the world is shifting to exploitation of heavy oil.

The fluid property that most greatly affects productivity and recovery is viscosity (Batzle et al 2006). The more viscous the oil, more energy needs to be injected into the system to reduce the viscosity to allow it to flow. Conventional oil viscosity can range from 1 centipoise (cP) [0.001 Pa*s] which is the viscosity of water, to about 10 cP [0.01 Pa*s]. Viscosity of heavy and extra-heavy oils can range from 10 cP [0.01 Pa*s] to 10,000 cP [10 Pa*s]. The most viscous hydrocarbon, bitumen, is a solid at room temperature and softens readily when heated. Viscosity of bitumen can range from 10,000 cP [10 Pa*s] to more than 1,000,000 cP [1,000 Pa*s] (Alboudwarej et al 2006). Figure 1 shows the logarithmic scale of viscosity subdivided by the grade category of oil, and compares it to the viscosities of typical items found in our kitchen. Figure 1 also illustrates the temperature-dependence of viscosity. Clearly, increasing reservoir temperature decreases the viscosity.
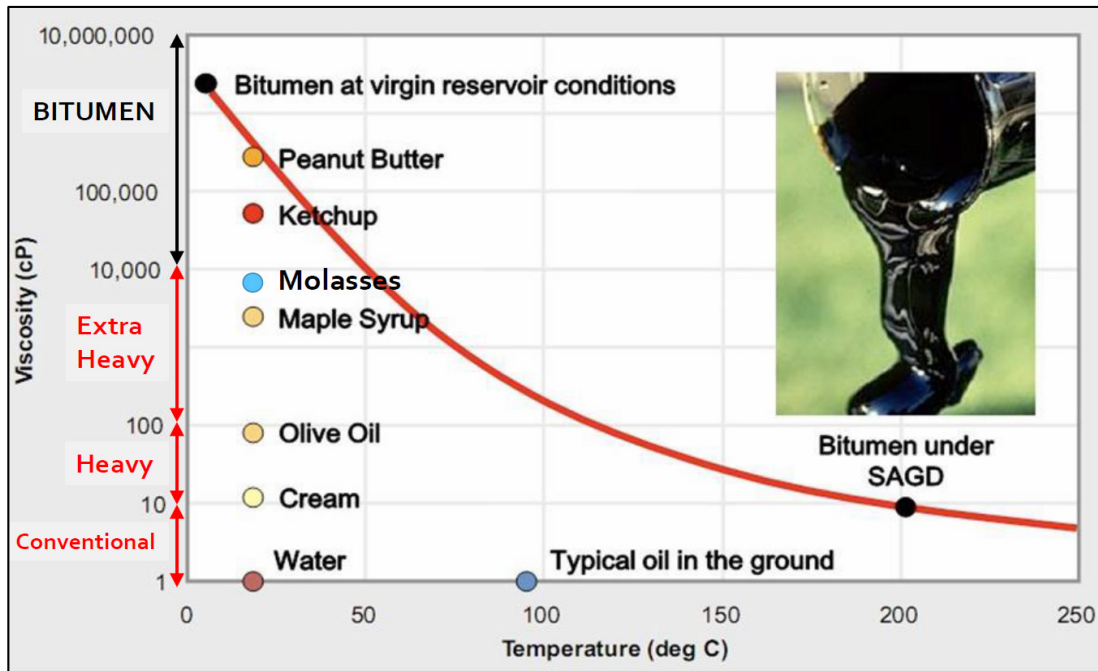
FIG. 1. Oil viscosities by grade category, compared to typical kitchen items. Note that viscosity has a logarithmic scale (ConocoPhillips Oil Sands website).

Figure 2 shows core plug measurements from the oil sands about 50 km south-southwest of Fort McMurray, Alberta (Kato et al. 2008). The measurements show that both Vp and Vs decrease with increasing temperature (or decreasing viscosity).
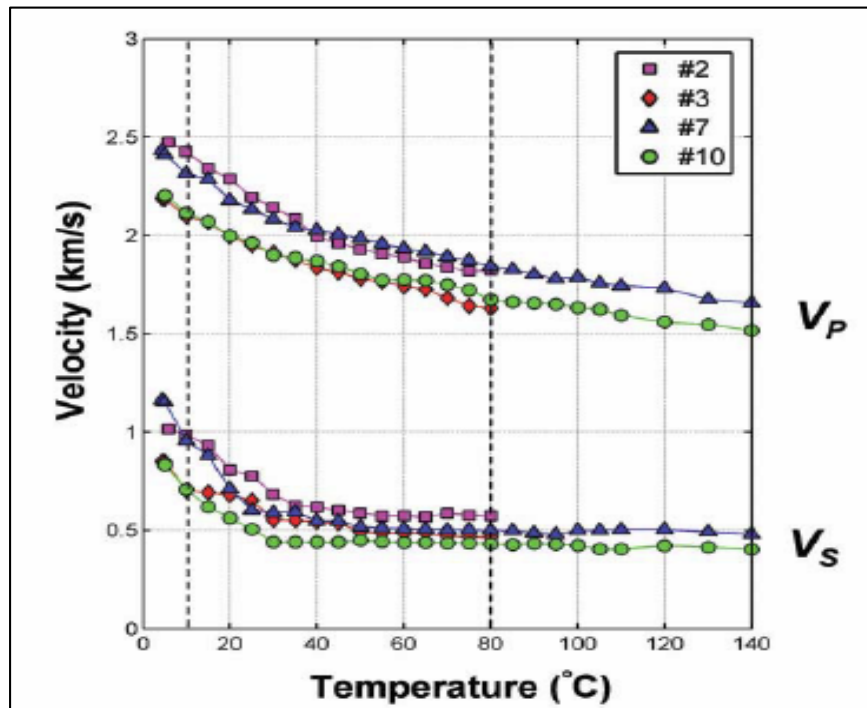

FIG. 2. P-wave and S-wave velocities of oil sands core plugs as a function of temperature at a constant pore pressure of 700 psi and confining pressure 900 psi (Kato et al. 2008).

In addition to its temperature dependence, measurements from Alberta oil sands operations indicate that viscosity also increases with reservoir depth. Figure 3 shows a depth-viscosity plot from ConocoPhillips's Surmont SAGD project, which is located only 10km south of the Athabasca South study area that this report is largely based on. It is not fully understood why bitumen viscosity increases with reservoir depth, but one of the proposed mechanisms is the increased biodegradation near the base of the reservoir due to the bottom-water (ConocoPhillips 2015).
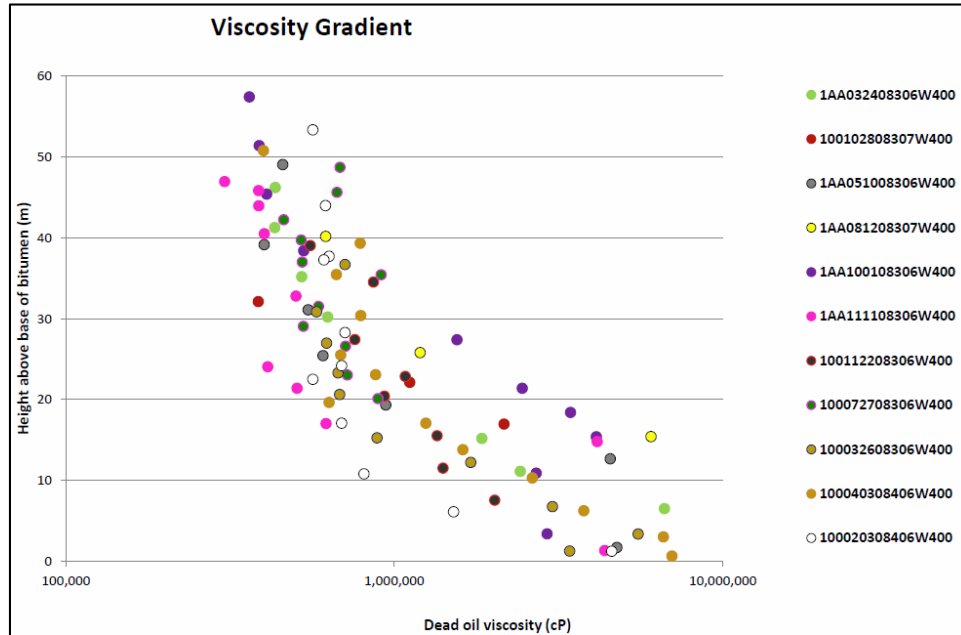

FIG. 3. Core sample viscosity measurements of the McMurray formation from ConocoPhillips's Surmont SAGD oil sands operation, located only 10km south of the Athabasca South project. This data shows that bitumen viscosity increases with depth in the McMurray formation (ConocoPhillips 2015).

Goal of this study

This study is an expansion of the work the author did in a previous CREWES report (Rops & Lines 2015), where it was demonstrated that viscosity could be predicted directly from well logs within 25% error. However due to the lack of publicly available viscosity data, the previous study was limited to a dataset of only 13 wells, with one viscosity measurement per well.

Donor Company has generously provided viscosity measurements for two of their oil sands development areas, with multiple measurements per well. The goal of this study is to establish a correlation between the measured viscosity values, and *all* of the available well log curves using multi-attribute analysis. Thanks to the large dataset provided by Donor Company, this study should also determine whether or not this geostatistical method of viscosity prediction is actually feasible.

THEORY – MULTI ATTRIBUTE ANALYSIS

The theory of multi-attribute analysis is explained in detail in a previous CREWES report in this volume (Rops & Lines 2015). A very brief summary is outlined here, with an additional section about the convolutional operator.

Figure 4 illustrates the basic multi-attribute problem, showing the target log and, in this case, three attribute logs to be used to predict the target attribute (Hampson-Russell 2013).
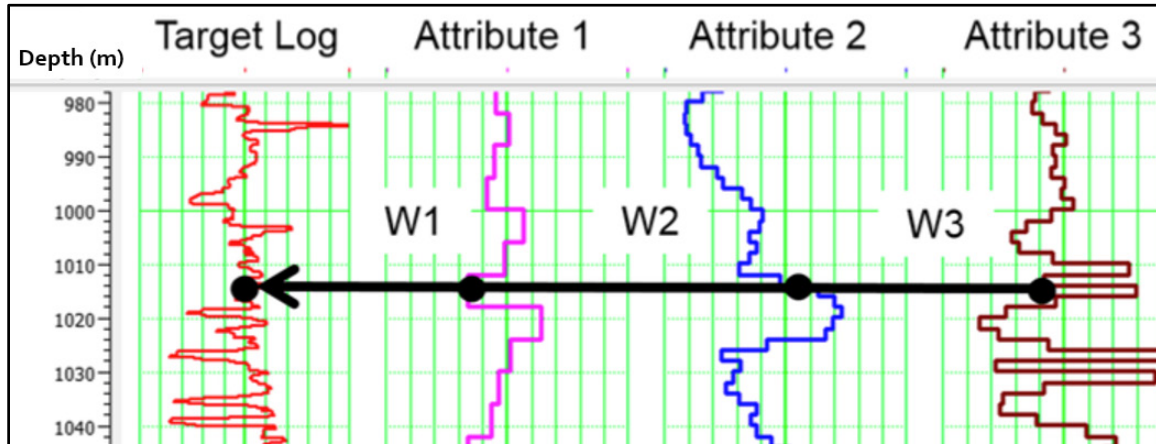

FIG. 4. The basic multi-attribute regression problem showing the target log and in this example, the 3 attributes to be used to predict the target (Hampson-Russell 2013).

To lay out the theory of multi-attribute prediction, let us assume that the target log is P-wave velocity, attribute 1 is bulk density, attribute 2 is gamma-ray, and attribute 3 is resistivity. The goal in this example is to predict P-wave velocity (in the depth domain) from the bulk density, gamma-ray, and resistivity curves.

We can write the fundamental equation for linear prediction as:

$$Vp(z) = w_0 + w_1 D(z) + w_2 G(z) + w_3 R(z) \tag{1}$$

where $Vp(z)$ is P-wave velocity in m/s, $D(z)$ is bulk density in kg/m^3, and $R(z)$ is resistivity in ohm*m. The regression coefficients $w_1, w_2 ...w_n$, can be solved for using least squares, and the best predictor attributes can be determined using a statistical method called step-wise regression (Russell 2004). Next, a method called cross-validation is used to determine how *many* attributes should be used to predict the target log (Russell 2004).

Please refer to Rops & Lines (2015) for a more complete explanation of the theory behind multi-attribute analysis.

The convolutional operator

The multi-attribute analysis explained so far correlates each target depth sample with the corresponding sample on each log attribute (as in Figure 4). By using a convolutional operator, each target sample is predicted using a weighted average of a group of samples on each attribute as shown in Figure 5 (Hampson-Russell 2013). For example, if the operator length is set to 5, then each target log sample will be predicted using weighted values of 5 neighboring samples on the attributes.
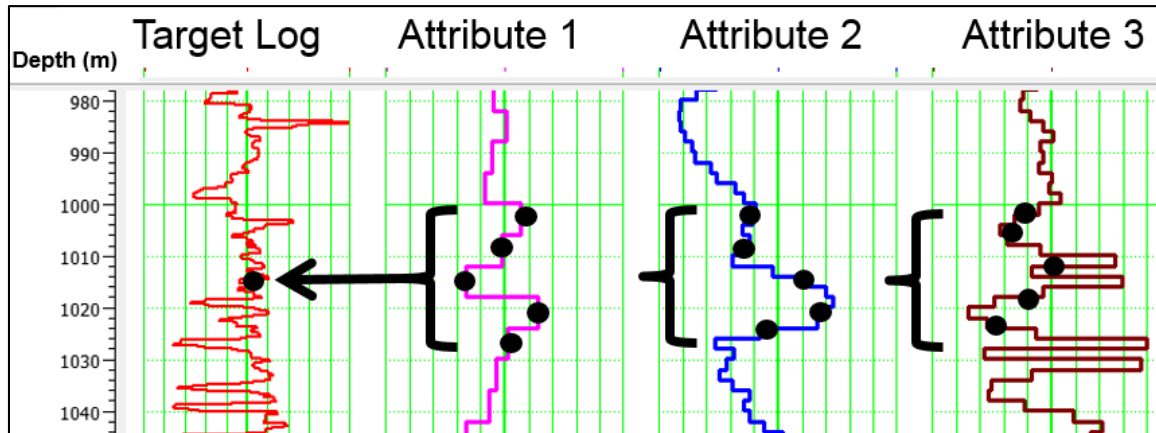

FIG. 5. Illustration of a 5-point convolutional operator, where 5 points for each attribute are averaged for every single point on the target attribute (Hampson-Russell 2013).

Instead of using Equation 1 to predict the target attribute, using a convolutional operator modifies the equation for linear prediction to look like:

$$Vp(z) = w_0 + w_1 * D(z) + w_2 * G(z) + w_3 * R(z) \qquad (2)$$

where "*" represents convolution by an operator (Hampson-Russell 2013).

Using the convolutional operator is like adding more attributes, it will always improve the prediction error, but the validation error may not improve and the danger of over-training is increased (Rops & Lines 2015). Figure 6 shows a validation error plot where 5 different operator lengths are used to predict P-wave velocity (Hampson-Russell 2013). In this example the validation error is minimized when a 7-point operator is used with 6 attributes, and using a 9-point operator over-trains the data.
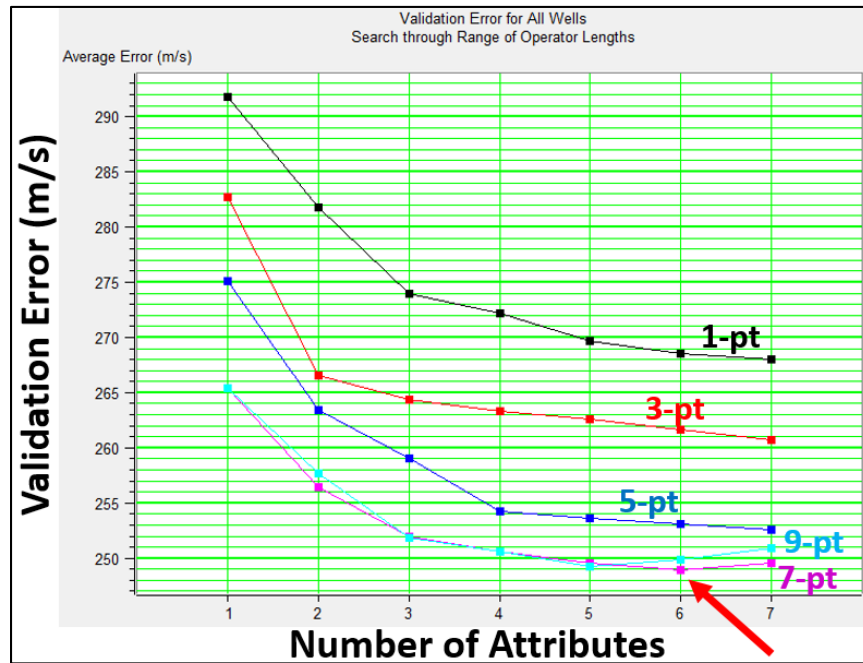
FIG. 6. Validation Error plot for 5 different operator lengths (Hampson-Russell 2013).

DATA AND RESULTS

The viscosity measurements used for this study were provided by Donor Company from their Athabasca North and Athabasca South oil sands projects. Figure 7a shows a regional map of where the projects are located. The wells each had cores taken from the McMurray formation. The bitumen was extracted from the cores by a 3rd party laboratory and the kinematic viscosities were measured at 35ºC, 55ºC, and 75ºC. The measurements at 35ºC were used for this study which most closely resembles reservoir conditions. Viscosity was measured in multiple intervals, ranging from 2 to 8 depth samples per well. The majority of wells had 3 viscosity measurements.

Athabasca North Data

Figure 7b shows a zoomed-in view of the Athabasca North project location. There are 24 wells in this area with viscosity measurements which have *all* of the well log attributes available in LAS format. The viscosities (measured at 35ºC) range from 35,000 cP to 802,000 cP, with an average measured viscosity of 229,000 cP. Note that the virgin reservoir conditions would be cooler than 35ºC, and the viscosities even higher.

In order to train a multi-attribute relation to predict viscosity from other logs, we need to have viscosity "logs" in the Hampson-Russell Emerge® database as well. Viscosity logs were manually created for each well by linearly interpolating the viscosities between each measurement point, and nulling the log everywhere outside of the reservoir interval. This is shown in Figure 8, where the six viscosity measurements are denoted by the red points, and the black curve is the interpolated viscosity log. The expected trend of viscosity increasing with depth is also apparent. The yellow areas highlight the training intervals,
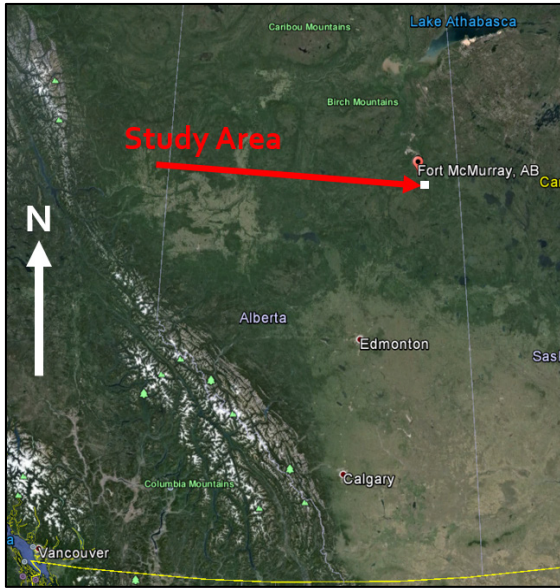
FIG. 7a. Location map of the Athabasca North and Athabasca South projects (Google Earth®).
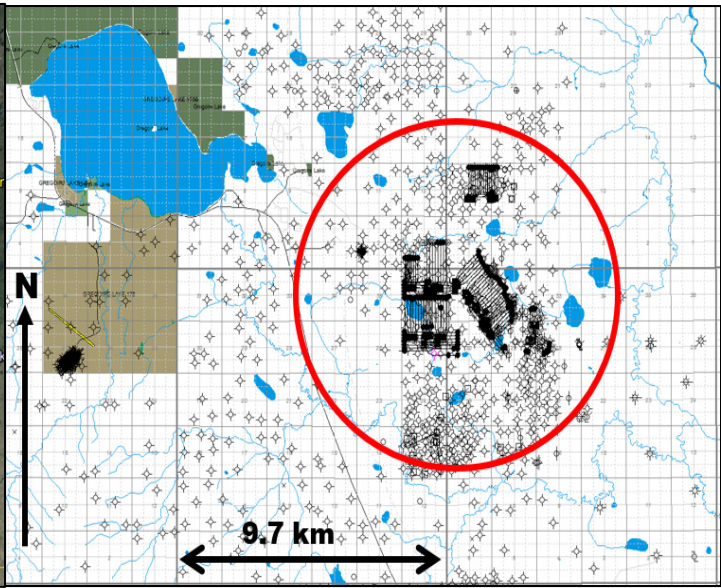
FIG. 7b. Zoomed-in view of the Athabasca North project area. All of the study wells are located within the red circle. Image from geoSCOUT®.
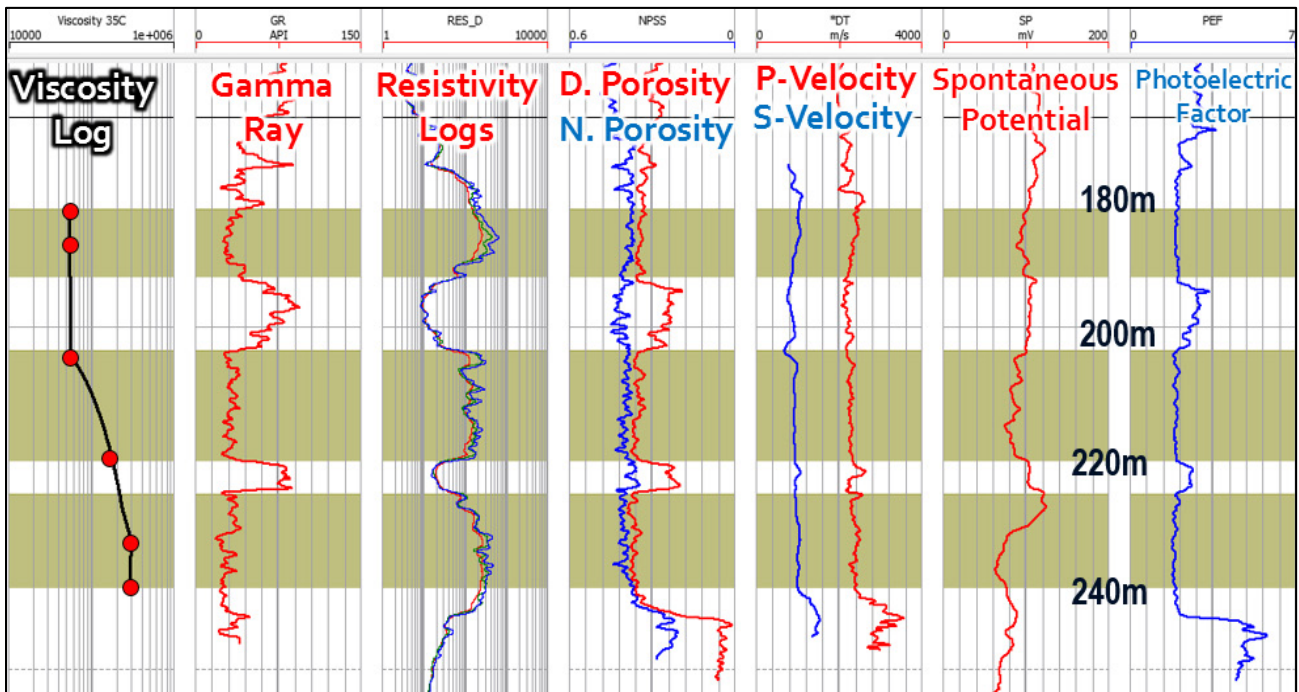
FIG. 8. Illustration of generating the viscosity "logs" and selection of the training intervals in one of the Athabasca North study wells. The red dots on the left are the provided viscosity measurements and the black curve is the interpolated viscosity log. Note that viscosity is presented on a logarithmic scale from 10,000 cP to 1,000,000 cP. The yellow areas highlight the training intervals (the mud barriers had to be avoided as shown).

and note that the mud barriers had to be avoided when selecting the training intervals. The low-permeability shale intervals act as barriers and do not contain bitumen, so if they were included in the training it would lead to highly erroneous viscosity predictions.

Figure 8 also serves as a nice example as a type-log for the Athabasca North area. The McMurray oil sands reservoir is a very clean sand as indicated by the low gamma-ray, and is very porous. From the porosity logs in the area, porosity ranges are between 30% and 40%. The high resistivity values indicate the presence of hydrocarbons, and unlike conventional oil settings there actually little separation between the resistivity logs due to the low invasion profile of the high viscosity oil sands (Rider & Kennedy 2011). Another key petrophysical difference between conventional and oil sands settings is the relative magnitudes of the resistivity logs. In conventional settings, resistivity logs are ordered such that Rdeep > Rmedium > Rshallow in hydrocarbon bearing intervals (Rider & Kennedy 2011). In bitumen settings, the shallow resistivity curve actually reads higher than the deep and medium curves (Rshallow > Rmedium > Rdeep). This is due to the low invasion profile of the drilling mud, and the tool measurement theory (Kevin Pyke, petrophysicist, personal communication, Nov 2, 2015).

Before the prediction results are presented, some notable issues with the well logs in Athabasca North should be mentioned. Figure 9 shows another example well, and there is frequent "criss-crossing" between the deep and shallow resistivity logs, which should not happen. The *S-wave sonic and SP* (spontaneous potential) logs throughout Athabasca North are also questionable (David Gray, personal communication, Oct 30, 2015). These issues could have an impact on the viscosity predictions in Athabasca North.
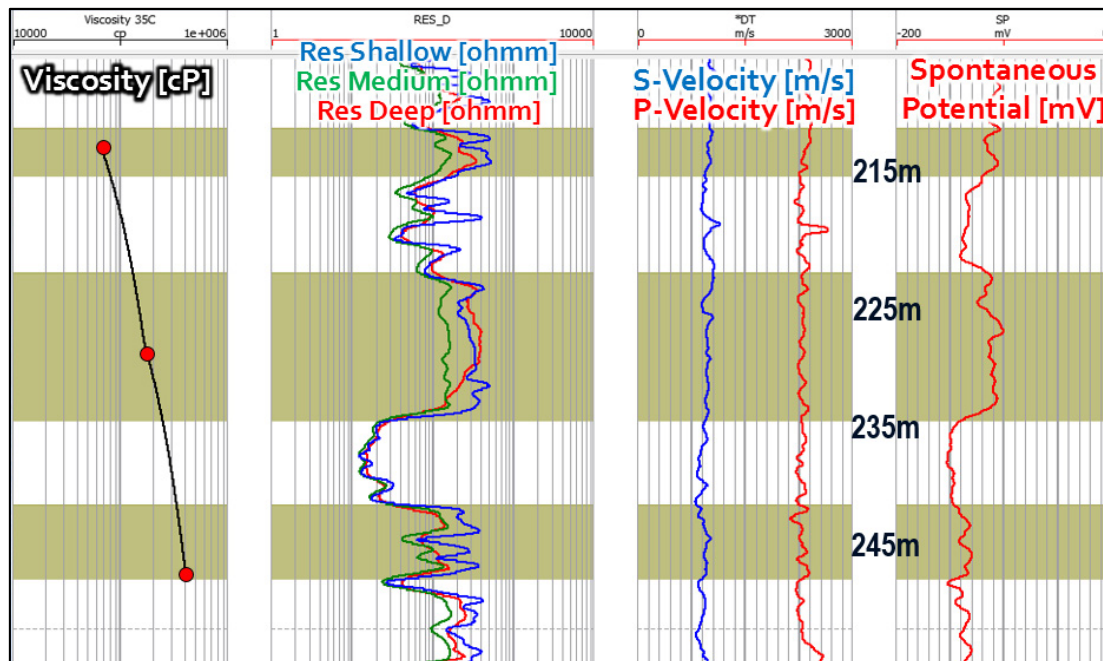

FIG. 9. Illustrating the issues with the resistivity logs in Athabasca North. The scales all increase from left to right, and the yellow areas highlight the training intervals. There is frequent "criss-crossing" between the deep and shallow resistivity curves, which is strange. The S-wave sonic and spontaneous potential logs are also questionable throughout Athabasca North (David Gray, personal communication, Oct 30, 2015).

Viscosity Prediction Results – Athabasca North

We will now use the multivariate procedure described in Rops & Lines (2015) to predict new pseudo-viscosity logs. The wells with *all* of the log attributes available in LAS format (24 wells) were used to train the train the relationship between viscosity and the well log attributes. Figure 10 shows the graphical training and validation errors of the multi-attribute analysis, along with the list of attributes used. Note that each row in the list corresponds to a particular multi-attribute transform *and includes all the attributes above it.* For example, the first row tells us that the best attribute to use is (1 / P-sonic [us/m]). The second row tells us that 1 / (P-sonic [us/m]) and (density porosity [%])^2 together is the best pair of attributes to use.
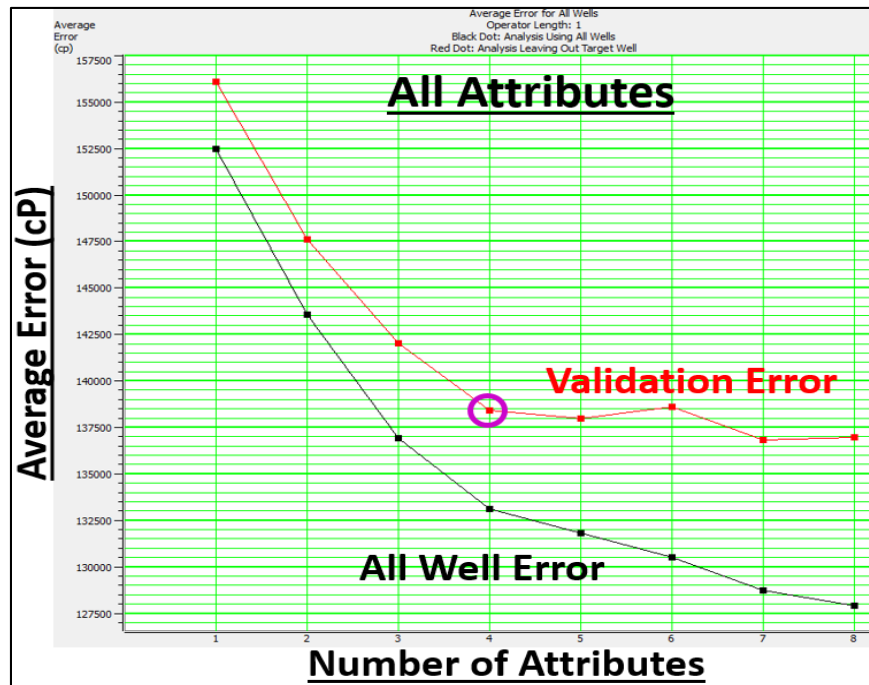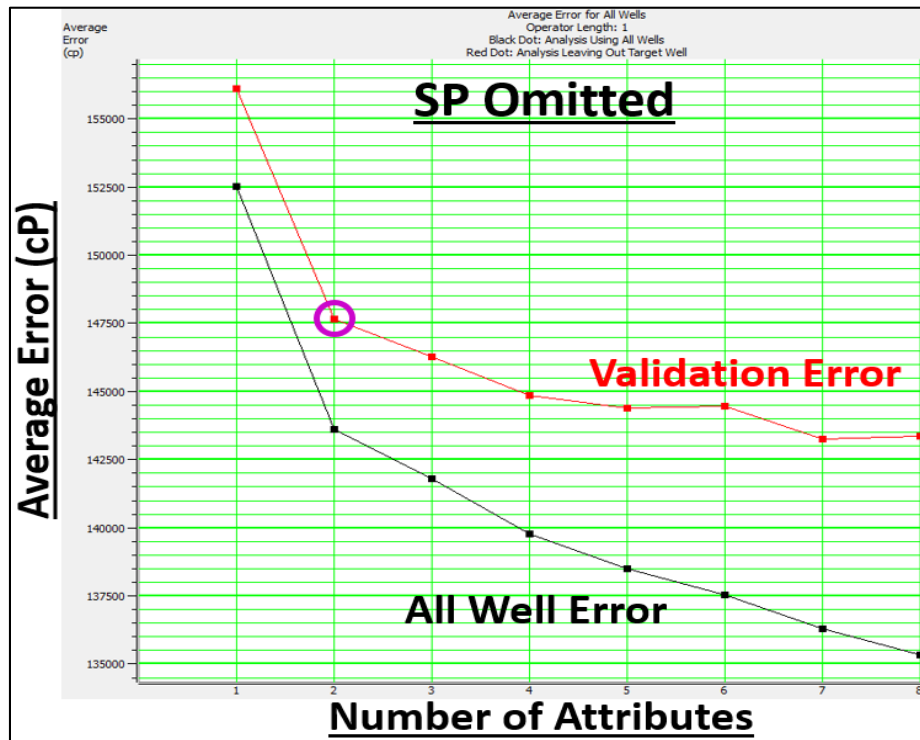

	Target (cP)	Final Attribute	Units	Validation Error (cP)
1	Viscosity	1 / (P-wave sonic)	1 / (μs/m)	156,138
2	Viscosity	(Density Porosity)^2	(decimal)^2	147,687
3	Viscosity	ln (SP)	ln(mV)	142,087
4	Viscosity	(Neutron Porosity)^2	(decimal)^2	138,472
5	Viscosity	Weight Percent Bitumen	decimal	138,035
6	Viscosity	ln (|Resistivity Separation|)	ln(ohmm)	138,673
7	Viscosity	Sqrt(Deep Resistivity)	Sqrt(ohmm)	136,868
8	Viscosity	1 / Caliper	1 / mm	136,998

FIG. 10. Emerge™ prediction error plot for viscosity (top), and the list of attributes with their associated validation errors (bottom). All of the well attributes from the 24 complete Athabasca North wells were used. The training error (all wells) is shown by the black dots and the validation error is shown by the red dots. Note that each row in the list corresponds to a particular multi-attribute transform *and includes all the attributes above it*.

Note that I combined both the error plot and the attribute list into a single figure (Figure 10). This is because they go directly hand in hand and to save space.

From Figure 10, the average validation error remains fairly flat at about 138,000 cP after seven attributes, which is 18% of the total viscosity range of the study wells. This tells us that an optimum fit between viscosity and our well logs is found by using the top four attributes in Table 1. Using any additional attributes risks over-training the relationship.

However, the results show that the SP (spontaneous potential) log is the third most important attribute to use. My first thought is that this does not make intuitive sense because SP does not have an absolute scale. Log analysts care about *relative* deflections of the SP curve (Rider & Kennedy 2011). Using an attribute without an absolute scale to predict absolute viscosity makes me nervous. Secondly, the SP logs in this area are questionable (David Gray, personal communication, Oct 30, 2015). The analysis was therefore modified to omit the SP log, and the updated results are displayed in Figure 11.

	Target (cP)	Final Attribute	Units	Validation Error (cP)
1	Viscosity	1 / (P-wave sonic)	1 / (μs/m)	156,138
2	Viscosity	(Density Porosity)^2	(decimal)^2	147,687
3	Viscosity	(Neutron Porosity)^2	ln(mV)	146,326
4	Viscosity	ln (|Resistivity Separation|)	(decimal)^2	144,903
5	Viscosity	sqrt(Weight Percent Bitumen)	sqrt(decimal)	144,430
6	Viscosity	1 / (S-P sonic difference)	1 / (μs/m)	144,507
7	Viscosity	1 / (VpVs Ratio)	unitless	143,287
8	Viscosity	1 / Caliper	1 / mm	143,388

FIG. 11. Emerge™ prediction error plot for viscosity (top), and the list of attributes with their associated validation errors (bottom). The 24 complete Athabasca North wells were used, with the SP log omitted from the analysis. The training error (all wells) is shown by the black dots and the validation error is shown by the red dots. Note that each row in the list corresponds to a particular multi-attribute transform *and includes all the attributes above it*.

From this result, it appears that the optimum viscosity prediction is done using the top two attributes: 1 / (P-sonic [*us/m*]) and (density porosity [*%*])^2. Beyond two attributes, even though there are small validation error improvements, there is also a higher risk of false correlations due to adding excess attributes (over-training). The average validation error using two attributes is about 147,000 cP, which is 19% of the total viscosity range of the study wells (35,000 cP to 802,000 cP). The prediction equation can be written as:

$$\eta = -2174261 + 851046336\left(\frac{1}{P - wave\ sonic}\right) + 3201332(DPSS)^2 \qquad (3)$$

where η is kinematic viscosity in centipoise (cP) at a specific depth sample, *P-wave sonic* is measured in μs/m, and *DPSS* is density porosity (sandstone matrix) as a fraction.

Figure 12 shows the prediction results for a good predictor well, a bad predictor well, and an average well plotted beside the logs used in the prediction. Each of the 24 wells were systematically left-out and predicted from the remaining 23 wells. The reservoir intervals are highlighted in yellow, which are the only intervals we care about, and all of the wells are scaled the same. In mud barriers between the reservoir intervals the viscosity predictions are nonsense, which is to be expected.

For the successful well (12b), P-velocity increases (or P-slowness decreases) with increasing viscosity as Equation 3 states. For the bad well (12a), P-velocity actually decreases in the bottom portion which could explain why the base reservoir prediction fails. For the density porosity predictor, no obvious visual trend relating to viscosity is present, however the log is much "noisier" in the bad predictor well (12a), and is more coherent and continuous in the successful prediction intervals (12b and 12c).

It is interesting that resistivity does not come up as an important viscosity predictor, since the first study of this method (Rops & Lines 2015) showed that resistivity was the second most important viscosity predictor. Resistivity is also sensitive to changing reservoir fluid types, so one might deduce that it should be a helpful viscosity predictor. The fact that resistivity did not come up as a predictor is likely a result of the questionable behavior of the resistivity logs in Athabasca North. Analysis of the wells from the Athabasca South project (next section) reveal how improved well data quality leads to better viscosity predictions.
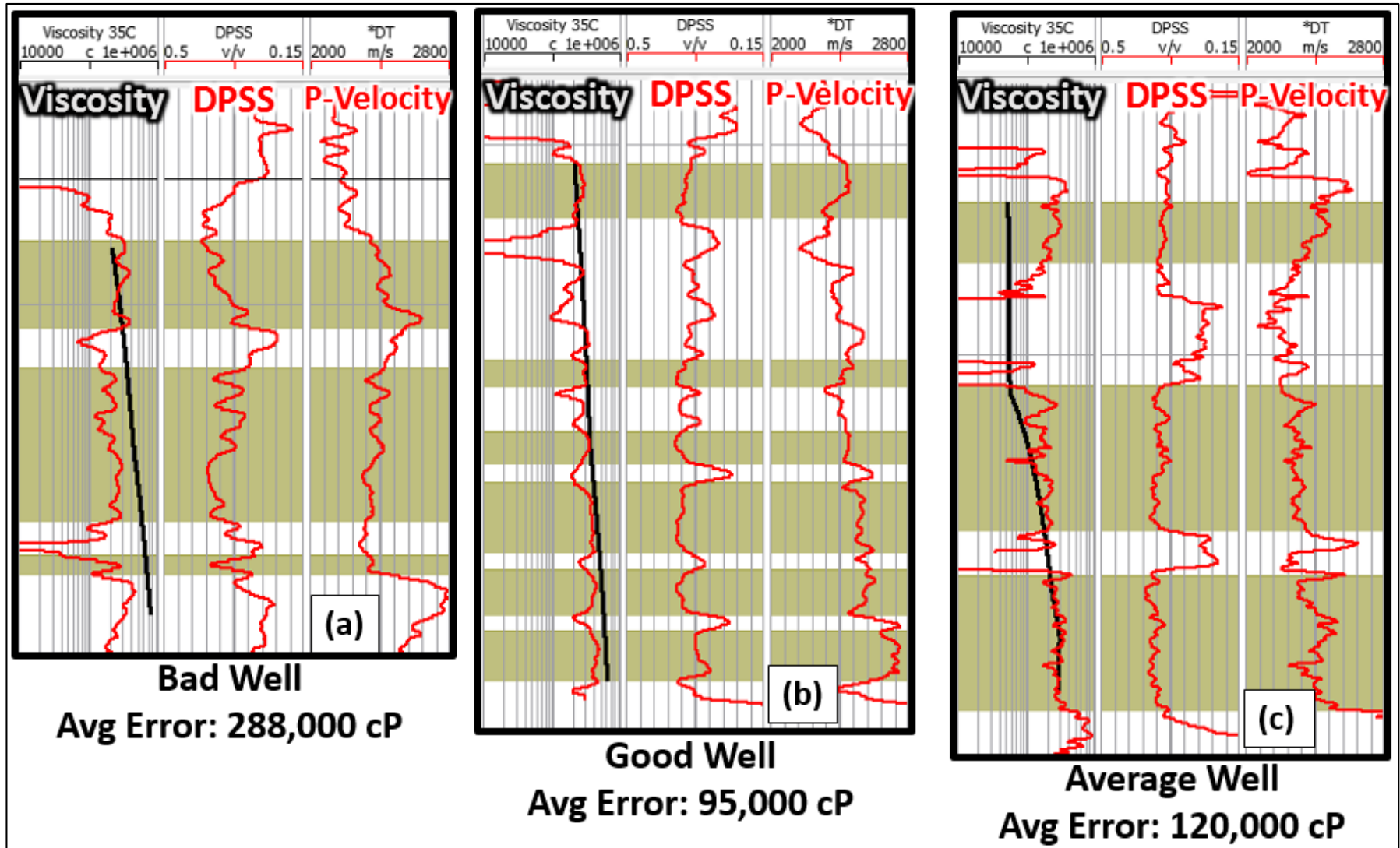
FIG. 12. Athabasca North viscosity prediction (validation) results for a bad predictor well (a), a good predictor well (b), and an average well (c). Each of the 24 wells were systematically left-out and predicted from the remaining 23 wells. The black curves in the viscosity tracks are the true (interpolated) viscosities and the red curves are the predicted viscosities using Equation 3. The logs used to predict viscosity are also plotted. The yellow areas highlight the reservoir intervals. The denoted errors are the average validation errors of each training interval within the well. Credit: Hampson-Russell Emerge™

Before moving on, an interesting exercise is to omit the top attribute from the analysis to see what the most important attributes would be in the absence of the top predictor. This is shown in Figure 13, where the P-wave sonic log was removed from the analysis.
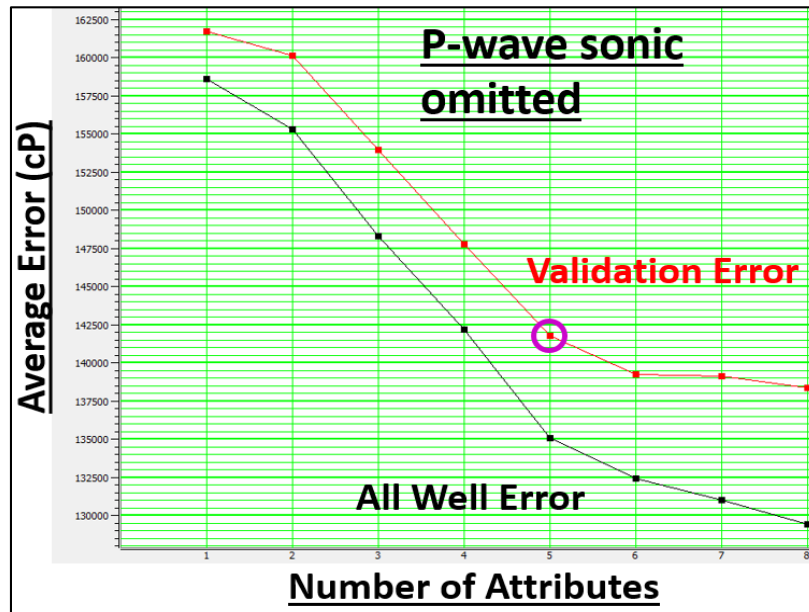
	Target (cP)	Final Attribute	Units	Validation Error (cP)
1	Viscosity	ln(Water Saturation)	ln(decimal)	161,753
2	Viscosity	1 / (S-wave sonic)	1 / (μs/m)	160,203
3	Viscosity	ln(S-P sonic difference)	ln(μs/m)	153,985
4	Viscosity	(Neutron Porosity)^2	(decimal)^2	147,845
5	Viscosity	ln(SP)	ln(mV)	141,846
6	Viscosity	(Density Porosity)^2	(decimal)^2	139,317

FIG. 13. Emerge™ prediction error plot for viscosity (top), and the list of attributes with their associated validation errors (bottom). The 24 complete Athabasca North wells were used, with the P-wave sonic log omitted from the analysis.

The validation errors have increased which is to be expected. However it is interesting that when P-wave sonic is dropped, the water saturation log rises to the top. Water saturation is a petrophysically-derived attribute which is directly related to the resistivity logs. The general form of the water saturation equation was defined by Archie (1941):

$$S_w = \sqrt{\frac{FR_w}{R_t}} \qquad (4)$$

where S_w is water saturation as a decimal, F is the formation resistivity factor (constant), R_w is the resistivity of the formation fluid in ohm*m, and R_t is the measured resistivity of the formation in ohm*m, which is often assumed to equal the deep resistivity log (Rider and Kennedy 2011).

The fact that water saturation is the second best single viscosity predictor suggests that the resistivity logs could actually be good viscosity predictors if they were better quality. It also suggests that bitumen saturation (S_o) could have a role in viscosity prediction, where $S_o = (1 - S_w)$.

Athabasca South Data

Figure 14 shows a zoomed-in view of the Athabasca South project location, which is located about 10km south of the Athabasca North project. Figure 15 shows a type-well in Athabasca South.
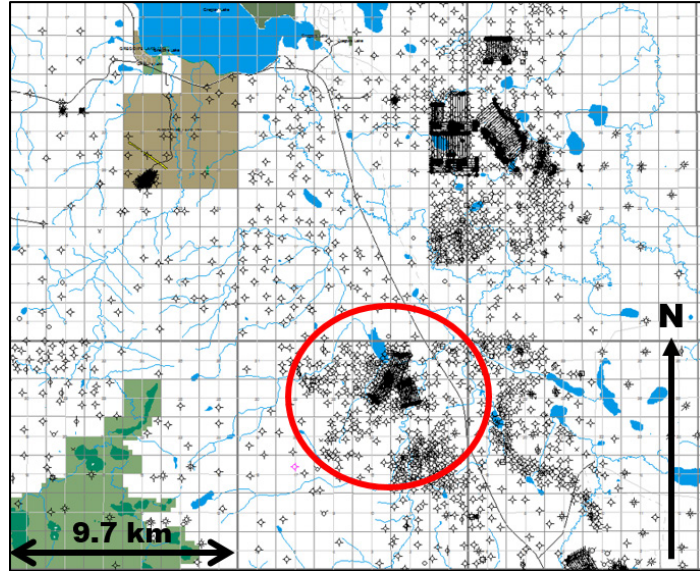

FIG. 14. Zoomed-in view of the Athabasca South project area. All of the study wells are located within the red circle. Image from geoSCOUT®.
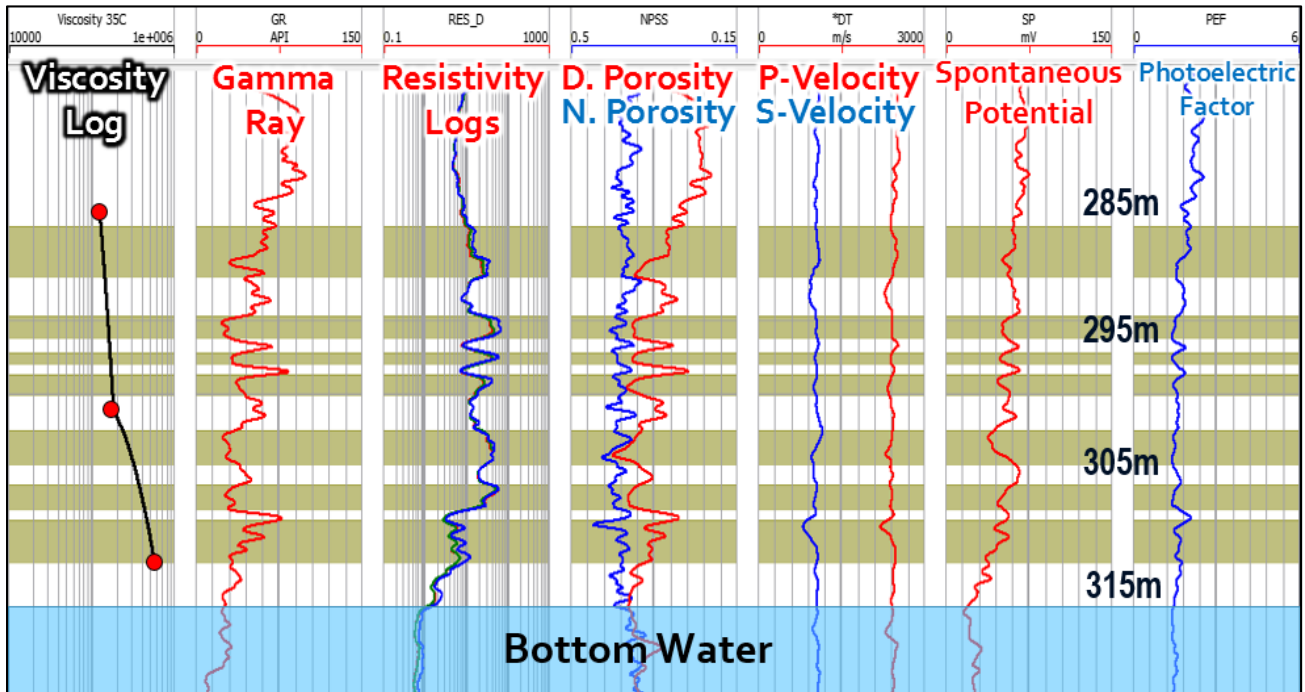

FIG. 15. Type well of the Athabasca South project area. The red dots on the left are the provided viscosity measurements and the black curve is the interpolated viscosity log. The viscosity is presented on a logarithmic scale from 10,000 cP to 1,000,000 cP. The yellow areas highlight the training intervals (the mud barriers had to be avoided as shown). There is bottom-water present at the base of the reservoir, based on the low resistivity, high porosity, and high sand content.

There are 40 wells in this area with viscosity measurements which have *all* of the well log attributes available in LAS format. The viscosities (measured at 35ºC) range from 9,000 cP to 550,000 cP, with an average measured viscosity of 121,000 cP. Note that the virgin reservoir conditions would be cooler than 35ºC, and the viscosities even higher.

Viscosity logs were manually created for each well by the same method as in Athabasca North, and illustrated in Figure 15. Similarly, the mud barriers were avoided when selecting the training intervals to avoid highly erroneous viscosity predictions. A notable qualitative difference in Athabasca South is that the resistivity logs appear more consistent than in Athabasca North. As in, the expected trend of Rshallow > Rmedium > Rdeep in bitumen saturated intervals was true most of the time, with the exception of a few intervals where the deep and shallow resistivity curves intersected. The medium resistivity curve consistently measured values between Rdeep and Rshallow in nearly all cases. Figure 15 also nicely illustrates the presence of bottom-water below the bitumen, which is believed to be a factor causing viscosity to increase with reservoir depth.

Viscosity Prediction Results - Athabasca South

We will now use the multivariate procedure described in Rops & Lines (2015) to predict new pseudo-viscosity logs in Athabasca South. The wells with *all* of the log attributes available in LAS format (40 wells) were used to train the train the relationship between viscosity and the well log attributes. The input attributes were: *caliper, density porosity (sandstone matrix), neutron porosity (sandstone matrix), effective porosity, neutron-density separation, P-wave sonic, S-wave sonic, S-P sonic separation, VpVs ratio, photoelectric factor (PE), gamma-ray, spontaneous potential (SP), medium resistivity, shallow-deep resistivity separation, water saturation,* and *weight percent bitumen.* The deep and shallow resistivity logs were omitted since the medium resistivity log was the most consistent.

Figure 16 shows the graphical training and validation errors of the multi-attribute analysis, along with the list of the attributes used. Note that each row in the list corresponds to a particular multi-attribute transform *and includes all the attributes above it.* This result shows that the optimum viscosity prediction can be done using the top four attributes, beyond that the validation error remains almost totally flat. The average validation error is about 72,000 cP, which is 13.3% of the total viscosity range of the study wells (9,000 cP to 550,000 cP).

The analysis so far has correlated each viscosity log value with the corresponding sample of each well log (ie. using an operator length of 1). We have not yet tried using a weighted average of the well logs (Figure 5) to predict viscosity. Figure 17 shows the prediction errors as a function of different operator lengths, using the same attributes as listed in Figure 16. From this result, the optimum viscosity prediction is found using the top four attributes with a 21-point operator, with an average validation error of **70,412 cP** (13.0% of the total viscosity range). In this case, an operator length of 21 has improved the viscosity prediction by 1,600 cP. Note that the 21-point operator starts to get unstable when using six or more attributes, which suggests that using an operator length any larger risks over-training the data.
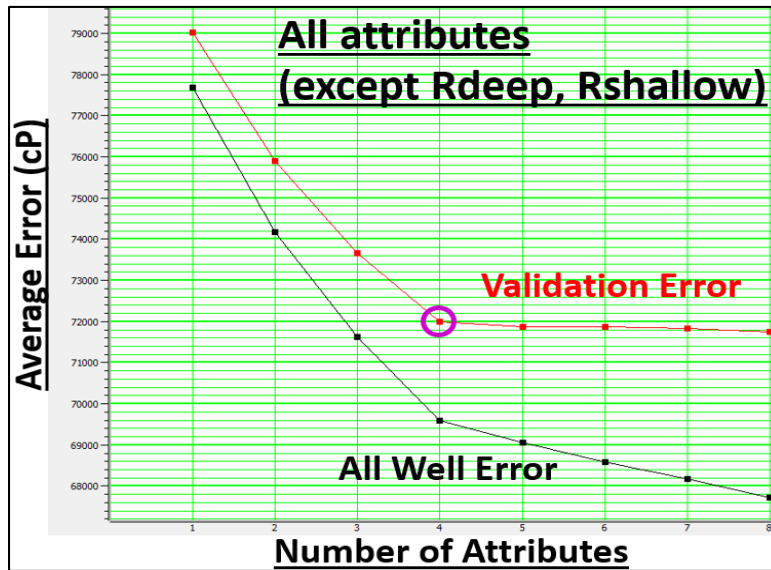
	Target (cP)	Final Attribute	Units	Validation Error (cP)
1	Viscosity	1 / (Medium Resistivity)	1 / (ohmm)	79,052
2	Viscosity	sqrt(Gamma Ray)	sqrt(API)	75,917
3	Viscosity	1 / (P-wave sonic)	1 / (μs/m)	73,673
4	Viscosity	ln (|Resistivity Separation|)	ln(ohmm)	72,022
5	Viscosity	ln(Spontaneous Potential)	ln(mV)	71,888
6	Viscosity	(Effective Porosity)^2	(decimal)^2	71,894
7	Viscosity	1 / (Water Saturation)	1 / (decimal)	71,857
8	Viscosity	Weight Percent Bitumen	decimal	71,775

FIG. 16. Emerge™ prediction error plot for viscosity (top), and the list of attributes with their associated validation errors (bottom). The 40 complete Athabasca South wells were used, with the deep and shallow resistivity logs omitted from the analysis. The training error (all wells) is shown by the black dots and the validation error is shown by the red dots. Note that each row in the list corresponds to a particular multi-attribute transform and includes all the attributes above it.
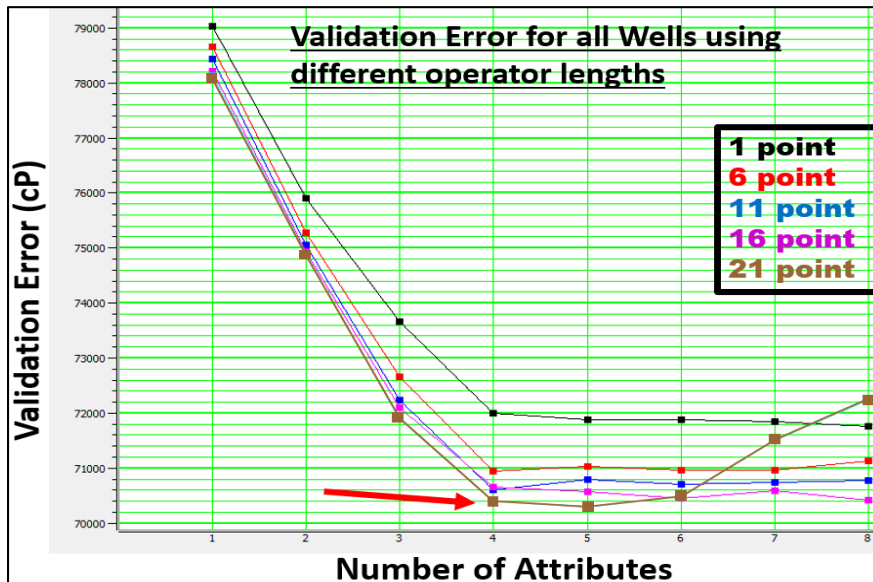

FIG. 17. Validation error plot for the 40 complete Athabasca South wells as a function of operator length. The validation error improves as the operator length increases for the range of lengths tested. The optimum prediction is achieved using 4 attributes and a 21-point operator.

The prediction equation using a 1-point operator (Figure 16) can be written as:

$$\eta = -96875 + 985321\left(\frac{1}{ResMedium}\right) - 31662\sqrt{GammaRay}$$
$$+ 176220384\left(\frac{1}{P-sonic}\right) - 10969ln(|ResSeparation|) \qquad (5)$$

where η is kinematic viscosity in centipoise (cP) at a specific depth sample, *ResMedium* is measured in ohm*m, *GammaRay* is measured in API units, *P-sonic* is measured in µs/m, and *|ResSeparation|* is the absolute value of the deep and shallow resistivity separation measured in ohm*m. The full prediction equation using a 21-point operator is found in Appendix A.

Figure 18 shows the prediction results for a good predictor well, a bad well where the base reservoir fails by about 230,000 cP, and an average well where the top reservoir somewhat fails by about 55,000 cP. Each of the 40 wells were systematically left-out and predicted from the remaining 39 wells. The reservoir intervals are highlighted in yellow, which are the only intervals we care about. In mud barriers between the reservoir intervals the viscosity predictions are meaningless.

For the successful wells (18b and 18c), resistivity decreases with increasing viscosity as Equation 5 states. For the bad well (18a), resistivity stays relatively constant which could explain why the base reservoir prediction fails. For the resistivity separation predictor, Well 18b has obvious separation and Well 18c does not, however both successfully predict the high viscosities at the base, suggesting that the separation may not be an important predictor after all. As for the Vp predictor, there is no obvious Vp increase (or P-slowness decrease) with increasing viscosity in Well 18b or Well 18c as Equation 5 states. However Vp seems to *decrease* with depth in Well 18a, which could also help explain the failed prediction at its base.

Similar to the exercise performed earlier for Athabasca North, the top predictor attribute (resistivity) was omitted from the analysis to see what the most important attributes would be in the absence of resistivity (Figure 19). The best predictor appears to be *ln(SP)* based on this result. SP measures natural electric potential differences and can detect permeability contrasts between beds (Rider & Kennedy 2011). It seems strange that SP is once again coming up as a predictor, because the SP log does not have an absolute scale. Log analysts care about *relative* deflections of the SP curve (Rider & Kennedy 2011).

In attempt to better understand this behavior, Figure 20 shows the viscosity predictions from Well 18c using only single attributes to better understand the dynamic behavior of the different predictors. Figure 20a shows the prediction using only *1/(Medium Resistivity [ohmm])*, which is clearly the most dynamic predictor (it predicts viscosity with the most detail). Figure 20b uses only *1/(P-sonic [µs/m])*, and Figure 20c uses only *1/(Gamma Ray [API])*, both of which appear to be less sensitive predictors than *1/(Medium Resistivity)*. Figure 20d uses only *ln(SP [mV])*, which simply predicts a relatively constant value. In other words, Figure 20d is basically saying that in the absence of a good quality predicting attribute, transform the SP log to a relatively-constant value that represents an average of all the known viscosities. For reference, the linear SP prediction equation is written as:
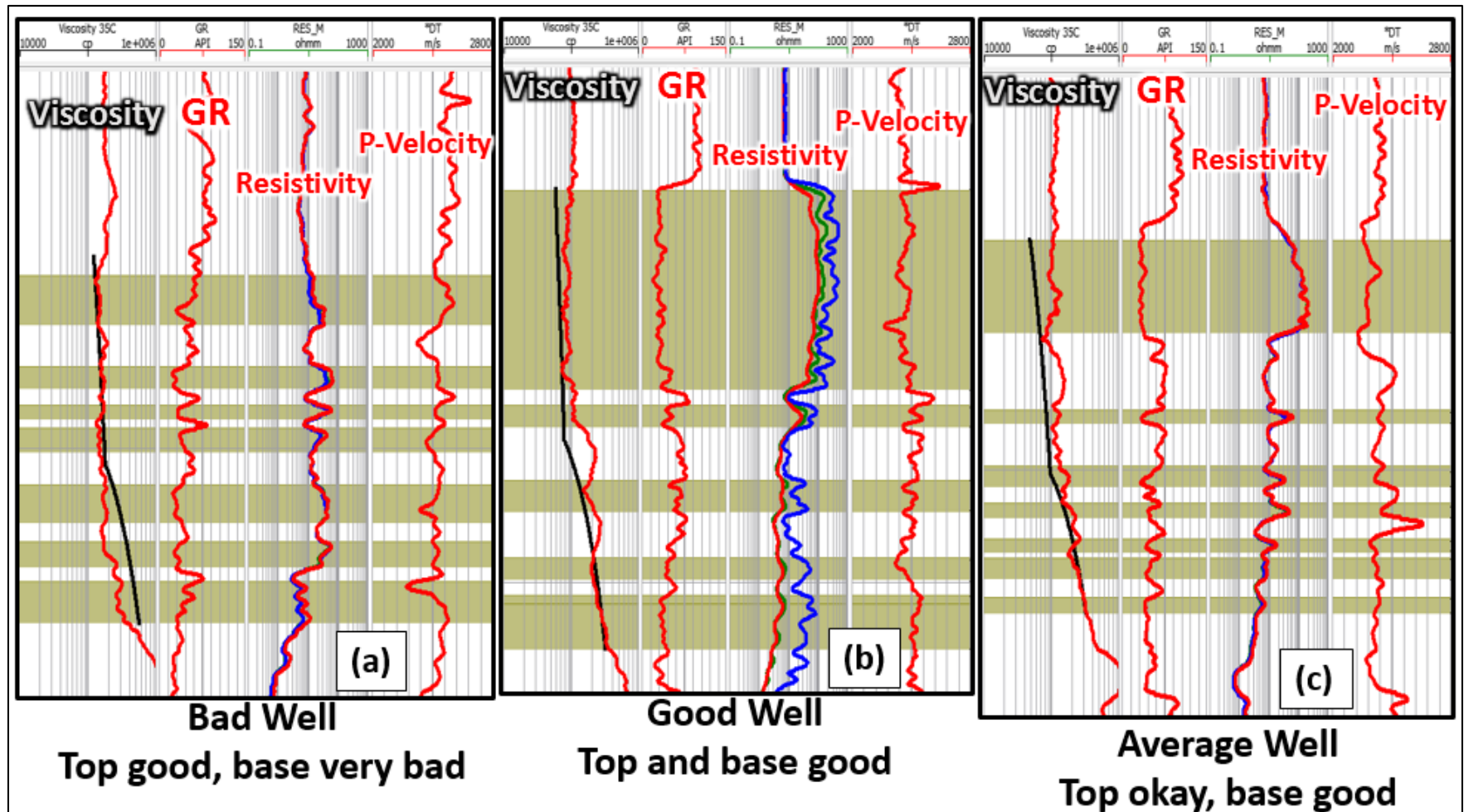
FIG. 18. Athabasca South viscosity prediction (validation) results for a bad predictor well (a), a good predictor well (b), and an average well (c). Each of the 40 wells were systematically left-out and predicted from the remaining 39 wells. The black curves in the viscosity tracks are the true (interpolated) viscosities and the red curves are the predicted viscosities using Equation A1. The logs used to predict viscosity are also plotted. The yellow areas highlight the reservoir intervals. Credit: Hampson-Russell Emerge™
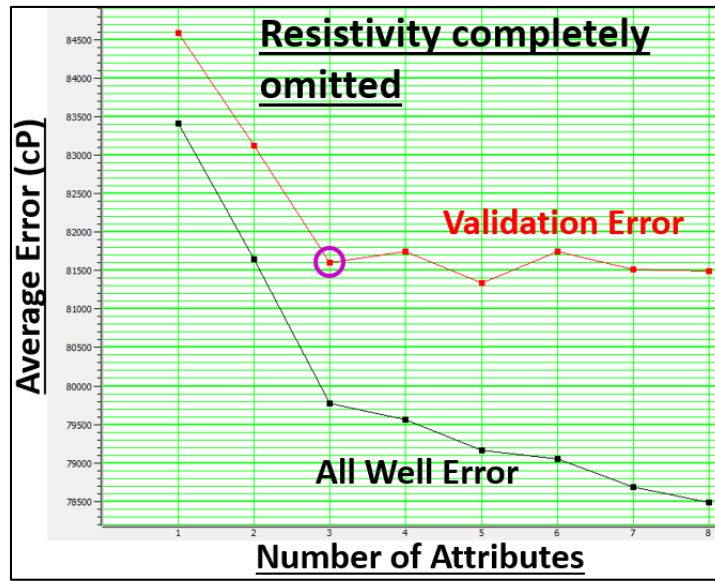
	Target (cP)	Final Attribute	Units	Validation Error (cP)
1	Viscosity	ln(Spontaneous Potential)	ln(mV)	84,600
2	Viscosity	1 / (Gamma Ray)	1 / API	83,136
3	Viscosity	1 / (P-wave sonic)	1 / (μs/m)	81,610
4	Viscosity	sqrt(S-wave sonic)	sqrt(μs/m)	81,752

FIG. 19. Prediction error plot for viscosity (top), and the list of attributes with their associated validation errors (bottom). The 40 complete Athabasca South wells were used, and the resistivity logs were completely omitted from the analysis.
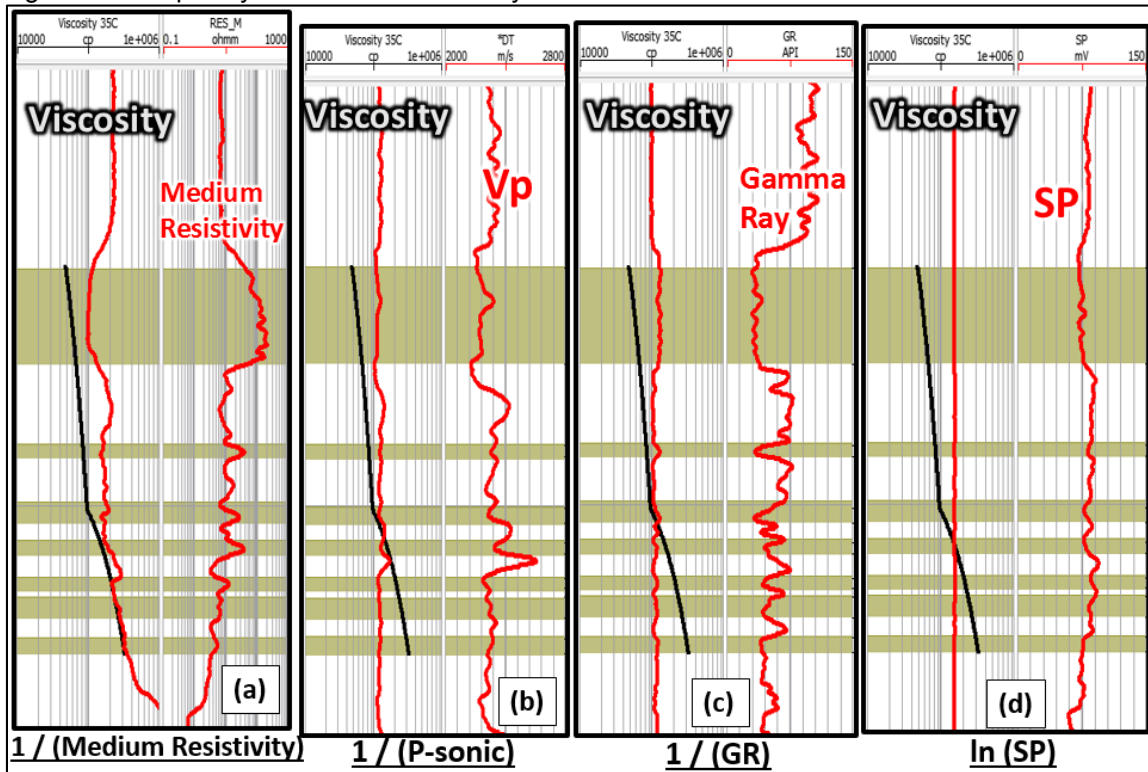

FIG. 20. Viscosity predictions for well 18c using only single attributes to see the dynamic behavior of the different predictors. (a) *1/(Medium Resistivity)* is used. (b) *1/(P-sonic [μs/m])* is used. (c). *1/(Gamma Ray)* is used. (d) *ln(Spontaneous potential)* is used. The black curves in the viscosity tracks are the true viscosities, and the red curves are the predicted viscosities.

$$\eta = 136944 + 4949ln(|SP|) \qquad (6)$$

where η is kinematic viscosity in centipoise (cP) at a specific depth sample, and *SP* is the spontaneous potential log measured in mV. The y-intercept is close to the average measured viscosity of the Athabasca South area, and the 2nd term corrects the prediction very slightly based on the SP log.

Comments about the predicting attributes

Comparing the prediction results between Athabasca North and Athabasca South, a common theme is that both the P-wave sonic and resistivity logs come up as top predictors (recall from Figure 13 that the water saturation log came up at the 2nd best solo predictor, which is directly related to the resistivity logs).

From the core plug measurements of Figure 2, both Vp and Vs decrease with increasing temperature (or decreasing viscosity). Since temperature and viscosity are closely related, it makes sense for Vp and Vs to be sensitive to viscosity variations as well. It is surprising that Vs never came up as a predictor, and that could be a result of the questionable quality of the shear sonic data in the project area. With better shear sonic data, the viscosity predictions would likely be improved further.

Resistivity logs are sensitive to changing reservoir fluid types, so it makes sense that resistivity came up as a viscosity predictor, although the exact mechanism is not known. The degree of bitumen saturation in the reservoir ($S_o = 1 - S_w$) from Equation 4 might also play a role in predicting viscosity in which case the resistivity of the formation water (R_w), which can change vertically and laterally, would become important. There is also a relationship between Vp and resistivity, first given by Faust (1953):

$$V_p = \gamma \left(Z \frac{R_0}{R_w} \right)^{1/6} \qquad (7)$$

where *Vp* is P-wave velocity in the fluid saturated rock in ft/s, γ is a constant, *Z* is depth in feet, R_0 is the resistivity of 100% water saturated rock in ohm*m, and R_w is the formation water resistivity in ohm*m. It is not clear yet whether the *separation* of the resistivity curves is a viable predictor due to the inconsistency of the deep and shallow resistivity logs in the project area.

Gamma ray came up as the second top predictor for Athabasca South (Figure 16). The gamma ray log measures the natural radioactivity of the formation, and is commonly used to calculate shale volumes and differentiate between sand units and shale units (Rider & Kennedy 2011). A physical reason why the gamma ray log would be related to viscosity is unclear, however gamma ray is related to other logs. For example, in reservoir intervals where gamma ray decreases, Vp tends to decrease, resistivity increases, and density decreases.

CONCLUSIONS AND FUTURE WORK

Multi-attribute analysis was successfully used to determine a relationship between bitumen viscosity and well logs in both the Athabasca North and Athabasca South project areas. In Athabasca North, *P-wave sonic* and *Density porosity* were used to predict viscosity and the average validation error for all wells was 147,000cP, or 19% of the total viscosity range. In Athabasca South, *medium resistivity, gamma ray, and P-wave sonic* were used to predict viscosity and the average validation error for all wells was only 70,000 cP, or 13% of the total viscosity range.

Sensitivity testing of the predicting attributes revealed that resistivity is the most dynamic viscosity predictor, in that it predicts viscosity with the most detail. P-wave sonic was shown to be a consistent but less dynamic predictor. In the absence of good predictors, it was found that, mysteriously, the SP log predicts the best average viscosity.

The importance of data quality was also observed. The resistivity, S-wave sonic, and SP logs in Athabasca North were of questionable quality, which was likely a factor as to why the validation errors in Athabasca North were twice as great as the validation errors in Athabasca South. However despite any influences from log data quality, both the P-wave sonic and resistivity logs came up as top predictors in both areas, and potential physical relationships to viscosity were briefly discussed.

Estimating viscosity ultimately adds value to any heavy oil or oil sands development project because it is used as a main criterion to select the optimum recovery method (Alboudwarej et al 2006). Viscosity is also used to refine production forecasts of heavy oil reservoirs once a recovery process has been selected (Miller et al 2006).

Future Work

With improved log data, the importance of the *separation* of the deep and shallow resistivity curves could be investigated in more detail, as well as the importance of the S-wave sonic log. Also, by incorporating estimates of how R_w varies throughout the area, the role of bitumen saturation in viscosity prediction could be investigated.

The next step I would like to try is using a neural network approach to predict viscosity (either a probabilistic, multi-layer, or discriminant analysis approach), which adds a whole new level of sophistication to the linear multi-attribute approach I have used.

It would also be interesting to see if depth and temperature could be incorporated into the viscosity predictions, given the strong evidence from previous studies of their relationships to viscosity.

ACKNOWLEDGEMENTS

REFERENCES

Alboudwarej, H., Felix, J., Taylor, S., Badry, R., Bremner, C., Brough, B., Skeates, C., Baker, A., Palmer, D., Pattison, K., Beshry, M., Krawchuk, P., Brown, G., Calvo, R., Triana, J., Hathcock, R., Koerner, K., Hughes, T., Kundu, D., Cardenas, J., & West, C. (2006). *Highlighting heavy oil*. Oilfield review, 18(2), 34-53.

Archie, G. E. (1941). *The electrical resistivity log as an aid in determining some reservoir characteristics*. Transactions of the AIME, 146(01), 54-62.

Batzle, M., Hofmann, R., & Han, D. H. (2006). *Heavy oils—seismic properties*. The Leading Edge, 25(6), 750-756.

Beggs, H. D., & Robinson, J. R. (1975). *Estimating the viscosity of crude oil systems*. Journal of Petroleum technology, *27*(09), 1140-1141.

Behura, J., Batzle, M., Hofmann, R., & Dorgan, J. (2007). *Heavy oils: Their shear story*. Geophysics, 72(5), E175-E183.

Bryan, J., Kantzas, A., & Bellehumeur, C. (2005). *Oil-viscosity predictions from low-field NMR measurements*. SPE Reservoir Evaluation & Engineering, *8*(01), 44-52.

Chopra, S., Lines, L. R., Schmitt, D.R., Batzle, M. (2010). *Heavy oils: reservoir characterization and production monitoring*. Society of Exploration Geophysicists.

ConocoPhillips AER Annual Performance Presentation (2015). Subsection 3.1.1 (2f), p.30. Accessed on November 12, 2015.
<http://www.aer.ca/documents/oilsands/insitupresentations/2015AthabascaConocoSurmontSAGD94609426.pdf>

De Ghetto, G., Paone, F., & ViIla, M. (1995). SPE 30316. *Pressure-Volume-Temperature Correlations for Heavy and Extra Heavy Oils*.

Faust, L. Y. (1953). *A velocity function including lithologic variation*. Geophysics, 18(2), 271-288.

Hampson-Russell (2013). *Emerge: Multi-Attribute Analysis* [Course notes].

Han, D. H., Liu, J., & Baztle, M. (2008). *Seismic properties of heavy oils—Measured data*. The Leading Edge, 27(9), 1108-1115.

Kato, A., Onozuka, S., & Nakayama, T. (2008). *Elastic property changes in a bitumen reservoir during steam injection*. The Leading Edge, 27(9), 1124-1131.

Miller, K. A., Nelson, L. A., & Almond, R. M. (2006). *Should you trust your heavy oil viscosity measurement?* Journal of Canadian Petroleum Technology, 45(4), 42-48.

Rider, M., & Kennedy, M. (2011). *The Geological Interpretation of Well Logs. 3rd Edition.* Rider-French Consulting Ltd., Glasgow, Scotland.

Rops, E. A., & Lines, L. R., (2015). *Predicting heavy oil viscosity from well logs – testing the idea*. CREWES Research Report, Vol 27 (**this volume)**.

Russell, B. H. (2004). *The application of multivariate statistics and neural networks to the prediction of reservoir parameters using seismic attributes*. Ph.D. thesis, Department of Geoscience, University of Calgary, Calgary, AB.

Shamsa, A., & Lines, L. (2014). *Effect of oil composition on fluid substitution in heavy oil reservoirs*. Geophysical Prospecting.

Vasheghani, F., & Lines, L. R. (2012). *Estimating heavy oil viscosity from crosswell seismic data*. Journal of Seismic Exploration, 21(3), 247-266.

APPENDIX A – FULL ATHABASCA SOUTH PREDICTION EQUATION

The full prediction equation for Athabasca South using a 21-point operator can be written as:

$$\eta = -156558 + w_1 * \left(\frac{1}{ResMedium}\right) + w_2 * \sqrt{GammaRay} + w_3 * \left(\frac{1}{P-sonic}\right)$$

$$+ w_4 * ln(ResSeparation) \tag{A1}$$

where η is kinematic viscosity in centipoise (cP) at a specific depth sample, "*" represents convolution by an operator, *ResMedium* is measured in ohm*m, *GammaRay* is measured in API units, *P-wave sonic* is measured in μs/m, and *ResSeparation* is measured in ohm*m. The regression coefficients w_1, w_2, w_3, w_4, are 21-point operators defined as:

w1	w2	w3	w4
739811.625	-18906.47266	75359600	-327.367889
-478696.5313	13414.67676	-25732600	-553.628723
-232349.4063	2750.363281	6364245.5	-521.89032
178064.6563	-5530.978027	12700955	-332.458069
218963.125	-5101.779297	2015255.75	413.83905
75623.21875	3.630725	-1916656.75	-878.481201
-38504.14063	-1242.518921	8501065	-1356.082642
-19402.44336	-1574.131958	9322693	-1289.851562
14391.60059	-4263.109375	43566476	-1623.327637
-5019.878906	-947.915955	-714875.125	-1315.029785
-3265.983643	-2668.846924	3748467.25	-548.245728
57937.41016	-2602.015625	-21597482	-472.381165
94691.45313	-2641.947998	-13700813	-494.663818
81574.13281	-1232.887207	11085149	-10.713683
86353.39844	-1884.713013	-7086170	318.605499
81566.33594	641.279114	12138783	-258.608398
115298.3438	-1930.737915	40417296	-305.841461
60659.97656	-1788.584351	40540524	-528.024475
-92642.77344	-1030.180054	-31138384	-1.072974
-159682.2969	1364.331909	-112925240	-392.900055
155465.5313	-2362.156494	165567248	-1896.943726